

RESEARCH ARTICLE

First Principle Investigation of Sr and Eu Doped $\text{La}_2\text{NiMnO}_6$: Structural, Electronic, Optical, Magnetic and Spintronics Properties

S. Firdous¹, G. F. A. Malik^{2,*}, N. Parveen³, F. A. Khanday², I. K. Pandey¹

ABSTRACT: This study investigates the effects of substituting $\text{La}_2\text{NiMnO}_6$ (LNMO) with Strontium (Sr) and Europium (Eu) dopants at the A-site, focusing on changes in material properties. Utilizing Density Functional Theory (DFT) with Local Density Approximation and Hubbard U Correction (LDA + U), we analyze the significant impact of these dopants on LNMO's optical, magnetic, electrical, and spintronic properties. Sr and Eu doping modifies the electronic structure of LNMO, enhancing its dielectric properties, which is crucial for applications requiring a high dielectric constant. The improved optical conductivity of doped LNMO makes it more efficient in light absorption and photoconductivity, beneficial for optoelectronic devices. Doping also enhances the magnetic properties of LNMO, advantageous for spintronics where spin control is essential. These dual improvements in electrical and magnetic properties suggest that Sr and Eu-doped LNMO are highly effective for energy storage technologies. Additionally, the mechanical properties of doped LNMO show improved resilience and stability, key indicators for the durability and longevity of devices. This comprehensive analysis highlights the potential of Sr and Eu-doped LNMO for advancements in spintronics, optoelectronics, and energy storage. The findings provide valuable insights into tuning material properties through doping, paving the way for synthesizing new multifunctional materials. This study not only enhances our understanding of the impact of dopants in double perovskites but also expands possibilities for innovative applications in high-tech fields, offering the potential for creating versatile materials and future innovations.

Keywords: Doping, Substitution, LNMO, Double Perovskite, Colossal Magnetoresistance.

Received: 28 March 2024; Revised: 17 May 2024; Accepted: 22 June 2024; Published Online: 17 July, 2024

1. INTRODUCTION

Since the inception of research in material science, Oxides have developed a significant interest in the minds of researchers due to its vast and diverse applications in the devices, strengthened by the fundamental Physics [1]. The oxides are different in nature be it acidic, basic, metallic, etc

[2]. Due to their broad category, they exhibit wide range of properties and functionalities, which make them crucial in scientific research as well as in technological applications [3]. The study of oxides has resulted in outstanding discoveries in phenomena like ferroelectricity, superconductivity, magnetism and multiferroicity, each opening new branches of exploration and innovation [1-4]. These materials play a pivotal role in the development of new advanced technologies generated from intrinsic properties and also from tuning up by various means essentially from doping, structural modifications and strain engineering, and so on [5]. One of the notable advantage of oxides over other materials (pure semiconductors and metals) are the cost effectiveness and the availability of the conventional processing methods [6]. The synthesis of oxides is quite simple and lower in cost which are beneficial for synthesis of large-scale applications

¹ Department of Chemistry, Singhania University, Rajasthan, India

² Department of Electronics and Instrumentation Technology, University of Kashmir, Jammu and Kashmir, India

³ Department of Electronics, Islamia College of Science and Commerce, Jammu and Kashmir, India

* Author to whom correspondence should be addressed:
gfarozam@gmail.com (G. F. A. Malik)

[7]. Their utilization is in various forms which includes bulk materials, polycrystalline powders, single crystals and thin films, each form is substantial for specific applications [8]. For instance, single crystals are often used in fundamental research to understand intrinsic material properties, while polycrystalline powders and thin films are more commonly used in practical applications such as capacitors, pyroelectric sensors, electro-optic devices, sensors, transducers, memory devices, and actuators [2-8].

One of the notable class of oxides is the perovskites, characterized by the general formula ABO_3 [6]. The unique geometry of perovskites, where a large cation A is surrounded by corner-sharing BO_6 octahedra, leads to a rich variety of physical properties [6]. Perovskites being ideal, where the positive and negative charge centers coincide perfectly, are rare. More commonly the centers imperfectly coincide each other resulting in overall net dipole moment and ferroelectricity [8]. The flexibility at the sites of A and B in the case of perovskite structure allows a path for wider range of Chemical compositions, accomplishing various diverse physical properties and multi-functionalities. The research on perovskites has not been beneficial only to understand the fundamentals of physics, but in an elaborative manner it provides the path for new related materials i.e. the double perovskites ($\text{A}_2\text{BB}'\text{O}_6$) [6, 9]. These materials have gained significant attention nowadays due to their lower cost production, utility and efficiency, which makes them prone in material research and innovations.

Double perovskites were developed to meet the growing needs of modern society [10-13]. These materials have the general formula $\text{A}_2\text{BB}'\text{O}_6$, where A is a divalent cation typically from alkaline or rare earth metals (f block elements), and B and B' are elements from alkali, alkaline, and d block elements [14]. The name "double perovskites" is derived from the repetition of perovskite cells, resulting in a rich variety of properties, including anti-ferromagnetism, half-metallicity, magnetoresistance, magneto-capacitance, and ferromagnetism [9-17]. These properties can be further tailored through various methods, such as doping or forming composites. Dopants can introduce new electronic states and alter the magnetic and electronic interactions in the materials, thereby tuning the properties for specific applications.

Double perovskites offer advantages in solar cell technology due to their wider diffusion lengths, high light absorption, and low processing temperature capabilities compared to silicon-based conventional cells. Notably, traditional silicon-based solar cells face challenges related to efficiency and toxicity, such as the presence of lead in lead-based perovskite solar cells [18]. Technological advancements have improved the efficiency of perovskite cells from 3.8% to 22.7% [19, 20], fueling further research into these compounds and their potential in photovoltaic technologies.

One prominent member of double perovskites is $\text{La}_2\text{NiMnO}_6$ (LNMO), known for its transition state around room temperature and magneto-dielectric behavior. LNMO has attracted significant interest due to its potential applications and physical properties [21]. Earlier studies

using density functional theory (DFT) indicated semiconducting behavior in LNMO [21, 22]. LNMO is ferromagnetic, while its end members, LaMnO_3 and LaNiO_3 , are antiferromagnetic and ferromagnetic, respectively. This combination of properties makes LNMO a fascinating material for further research [21-31].

$\text{La}_2\text{NiMnO}_6$ exhibits two phases due to temperature changes: monoclinic at room temperature and rhombohedral at higher temperatures, indicating a phase transition influenced by atmospheric conditions and temperature [23, 24]. Altering the physical properties of double perovskites through substitutional doping is an area of ongoing research. Substituting different cations at the A-site affects the physical properties, considering factors like ionic radii, valencies, and oxidation states [24]. These substitutions alter the B-O-B angles, influencing the material's electronic structure and magnetic properties. For example, Wang Ting et al. reported that doping with calcium introduces antiphase defects, increasing antiferromagnetic anti-phase boundaries and enhancing long-range ferromagnetic order near the transition point [25, 26]. Gadolinium doping enhances the insulating behavior of the material, demonstrating how different dopants can enhance the properties of double perovskites for specific applications.

Many materials, including perovskites and carbon nanotubes, have been doped using DFT to predict and improve their performance [27]. However, achieving simulated results experimentally remains a significant challenge. Despite the ease of synthesizing double perovskites, practical applications face issues like stability and efficiency. For light-harvesting materials, cost and toxicity are significant concerns, particularly for silicon-based and lead-halide-based perovskite solar cells [28, 29]. Researchers have turned to alternative materials and novel synthesis methods to overcome these drawbacks. For instance, Kumar et al. synthesized a heterostructure of LNMO and TiO_2 using simulation methods, achieving a power conversion efficiency of up to 15.42% [27]. Similarly, inorganic lead-free perovskite oxides with bandgap variations of 1.08 to 1.19 eV have been synthesized, achieving higher carrier lifetimes compared to halide-based perovskite cells and comparable to silicon-based solar cells [28]. These features highlight the potential of perovskite materials in developing efficient and environmentally friendly photovoltaic technologies [27, 28]. Lan et al. reported that the monoclinic phase of LNMO is preferable for light-harvesting applications compared to other phases [29]. The current research provides insights into the monoclinic phase for solar cell use while performing substitutional doping to enhance light response. The optical delineation of doped LNMO results in significant improvements in light absorption and conductivity in the visible spectrum, suggesting its viability for solar and energy storage devices [29].

This paper explores the optical properties of $\text{La}_2\text{NiMnO}_6$ (LNMO) doped with Strontium (Sr) and Europium (Eu), highlighting their significant impact on the material's characteristics. Using Density Functional Theory (DFT) with

LDA + U corrections, we found that doping enhances LNMO's potential in the electronic industry, specifically in photonics, energy storage, and spintronics. These dopants lead to the creation of multifunctional, exotic materials with improved properties.

Double perovskites, known for their diverse applications including magnetism, optoelectronics, and catalysis, make LNMO a promising candidate due to its excellent ferromagnetic and semiconducting properties. Our study focuses on how Sr and Eu doping at the A-site affects LNMO's optical, magnetic, spintronic, electrical, and mechanical properties. Doping with Sr, which has a larger ionic radius than La, expands the lattice and modifies bond angles, enhancing ferromagnetic and semiconducting behavior by affecting the electronic band structure and magnetic interactions. On the other hand, Eu, with a smaller ionic radius but higher valency, introduces significant electronic perturbations and new magnetic interactions, crucial for spintronics applications.

We utilized DFT to capture the magnetic and electronic correlations within the doped LNMO system, analyzing changes in the electronic band structure, magnetic properties, and density of states to understand the mechanisms driving property modifications. Additionally, we evaluated the optical properties of the doped LNMO, focusing on light absorption and conductivity, which are essential for developing photovoltaic and optoelectronic applications. Mechanical stability was also assessed, as it is vital for the durability and performance of devices.

Our comprehensive analysis aims to provide a detailed understanding of Sr and Eu-doped LNMO, revealing their potential for applications in spintronics, photovoltaics, and energy storage. This study advances our knowledge of double perovskites and sets the stage for future research and development of advanced materials with tailored properties, pushing the boundaries of material science and fostering technological innovation.

2. COMPUTATIONAL DETAILS

2.1. Computational Details

For the computational details, we employed the Vienna Ab initio Simulation Package (VASP) for all calculations related to Density Functional Theory (DFT). The projector-augmented wave (PAW) method was used to describe the electron-ion interactions accurately. This method allows for a more precise representation of the wavefunctions near the atomic cores. The exchange-correlation potential was treated within the Local Density Approximation plus Hubbard U (LDA + U) framework. The LDA + U approach is essential for accounting for the strong on-site Coulombic interactions in the d-orbitals of d-block elements, which are crucial for correctly describing the electronic structure of materials with strongly correlated electrons.

2.2. Structural Optimization

The initial structures of $\text{La}_2\text{NiMnO}_6$, Sr-doped $\text{La}_2\text{NiMnO}_6$ ($\text{La}_{1.9}\text{Sr}_{0.1}\text{NiMnO}_6$), and Eu-doped $\text{La}_2\text{NiMnO}_6$ ($\text{La}_{1.9}\text{Eu}_{0.1}\text{NiMnO}_6$) were fully optimized to achieve stable configurations. The optimization process continued until the forces acting on each atom were reduced to less than 0.01 eV/Å. This ensures that the structures are at their minimum energy configurations. A Monkhorst-Pack k-point mesh of $6 \times 6 \times 6$ was used for sampling the Brillouin zone, which provides a good balance between computational cost and accuracy. A plane-wave cutoff energy of 500 eV was used, ensuring that the wavefunctions were well-represented. Figure 2 illustrates the density of states (DOS) for monoclinic $\text{La}_2\text{NiMnO}_6$, providing insights into the electronic structure of the material.

2.3. Electronic Structure and Optical Properties

The electronic structure, including the density of states (DOS) and band structures, was computed to understand the impact of Sr and Eu doping on $\text{La}_2\text{NiMnO}_6$. The DOS helps identify the distribution of electronic states across different energy levels, while the band structure reveals the material's conductive properties by showing the energy bands. To investigate the optical properties, we derived the dielectric function, refractive index, and absorption spectra from the frequency-dependent complex dielectric function. These properties are critical for assessing the material's potential in optoelectronic applications, as they determine how the material interacts with light across different wavelengths.

2.4. Magnetic and Spintronic Properties

The magnetic properties were investigated by calculating the total and partial magnetic moments of the doped and undoped $\text{La}_2\text{NiMnO}_6$ structures. Spin-polarized calculations were performed to analyze the potential of Sr and Eu-doped LNMO for spintronic applications. These calculations help in understanding how doping influences the spin alignment and magnetic ordering within the material, which is crucial for applications in spintronics, where the control of electron spin is used to store and transfer information.

2.5. Mechanical Properties

To evaluate the mechanical stability and rigidity of the doped structures, we computed the elastic constants. These constants include the bulk modulus, shear modulus, and Young's modulus, which were derived from the elastic constants. The bulk modulus measures the material's resistance to uniform compression, the shear modulus indicates resistance to shear deformation, and Young's modulus reflects the stiffness of the material. Understanding these properties is essential for assessing the material's

suitability for various applications, particularly those involving mechanical stress and strain. The comprehensive methodology ensures a detailed understanding of how Sr and Eu doping influences the structural, electronic, optical, magnetic, spintronic, and mechanical properties of $\text{La}_2\text{NiMnO}_6$. The insights gained from these studies are crucial for developing advanced materials with tailored properties for specific high-performance applications.

3. RESULTS AND DISCUSSION

3.1. Structural Properties

Figure 1 visually represents the impact of different dopants on the LNMO structure, highlighting how doping can alter its physical properties and enhance its suitability for various applications. Figure 1 illustrates the structural variations in $\text{La}_2\text{NiMnO}_6$ (LNMO) under different doping conditions. Figure 1 (a) shows the undoped $\text{La}_2\text{NiMnO}_6$, representing the pristine structure of LNMO without any dopants. The crystal lattice and atomic arrangement reflect the default state of the material, providing a baseline for comparison with doped variants. Figure 1 (b) depicts the LNMO structure after doping with Strontium (Sr). Doping with Sr, which has a larger ionic radius than La, is expected to expand the lattice structure and alter bond angles. These changes can modify the electronic band structure and magnetic interactions, potentially enhancing the material's ferromagnetic and semiconducting properties. Figure 1 (c) shows the LNMO structure doped with Europium (Eu). Eu, having a smaller ionic radius than La but a higher valency, introduces significant electronic perturbations. These changes affect the electronic density of states and magnetic exchange

interactions, which are crucial for applications in spintronics.

The structural properties of $\text{La}_2\text{NiMnO}_6$ (LNMO) and its Sr and Eu-doped variants were thoroughly investigated through structural optimization. The optimized lattice parameters for the undoped and doped compounds are summarized in Table 1. These parameters include the lattice constants a , b , and c , which define the dimensions of the unit cell in the crystal structure. The substitution of La with Sr and Eu leads to slight changes in the lattice constants, indicating successful incorporation of the dopants into the LNMO structure. Specifically, the lattice constants a and b show a minor increase when Sr is introduced (from 5.54 Å to 5.56 Å), while the introduction of Eu results in a similar yet slightly smaller increase (to 5.55 Å). The lattice constant c also increases slightly for both dopants, with Sr-doped LNMO showing a more significant increase (from 7.81 Å to 7.83 Å) compared to Eu-doped LNMO (to 7.82 Å).

These changes in lattice parameters are crucial as they reflect the dopants' impact on the crystal structure of LNMO. The increase in lattice constants suggests that the dopants cause an expansion of the unit cell. This expansion can be attributed to the differences in ionic radii between La, Sr, and Eu. Sr has a larger ionic radius compared to La, leading to a more pronounced expansion in the lattice. In contrast, Eu has an ionic radius similar to La, resulting in a less significant increase in lattice dimensions [28].

Furthermore, the successful incorporation of Sr and Eu into the LNMO lattice without disrupting the overall crystal structure confirms the stability of the doped compounds. This stability is essential for maintaining the material's integrity and ensuring consistent performance in various applications. The slight variations in lattice parameters due to doping can also influence the electronic and magnetic properties of LNMO. Changes in the crystal structure can affect the overlap between atomic orbitals, thereby altering the electronic band structure and magnetic interactions.

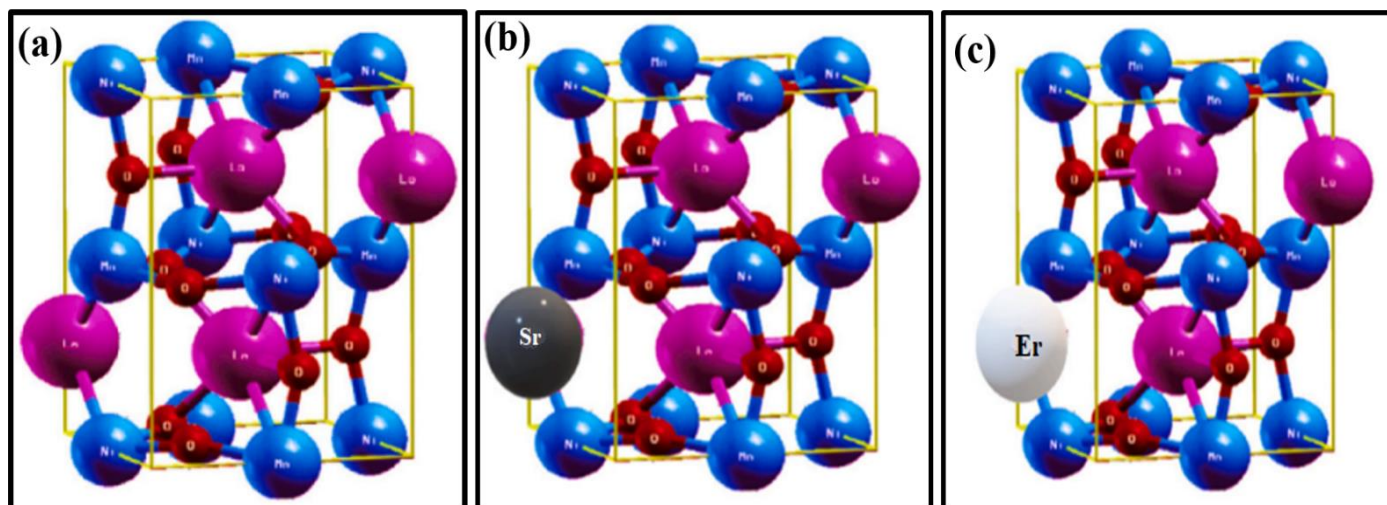


Fig. 1. Structure of $\text{La}_2\text{NiMnO}_6$: (a) undoped $\text{La}_2\text{NiMnO}_6$, (b) Sr-doped $\text{La}_2\text{NiMnO}_6$, (c) Eu-doped $\text{La}_2\text{NiMnO}_6$.

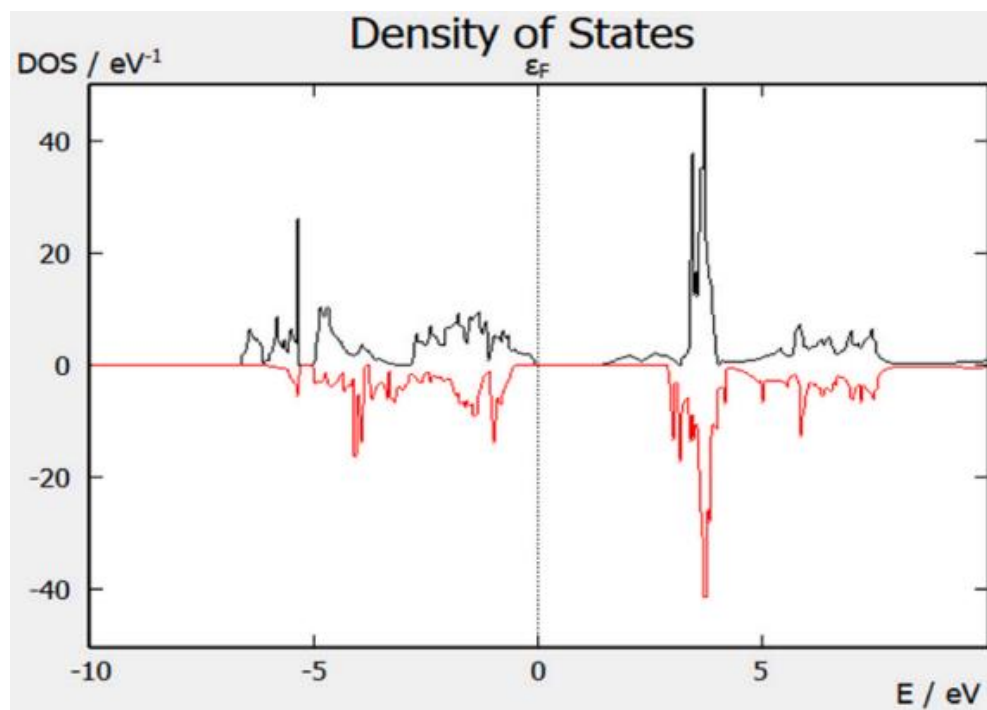


Fig. 2. Density of States (DOS) of Monoclinic $\text{La}_2\text{NiMnO}_6$.

Therefore, understanding these structural modifications is a critical step in comprehensively analyzing the dopants' effects on LNMO's overall properties. The optimized lattice parameters for $\text{La}_2\text{NiMnO}_6$ and its Sr and Eu-doped variants demonstrate successful doping and slight expansions in the crystal lattice. These structural changes set the stage for further investigation into how these modifications impact the material's electronic, magnetic, and other functional properties, which will be discussed in subsequent sections. **Figure 2** exhibits the density of state (DOS) graph for the monoclinic $\text{La}_2\text{NiMnO}_6$.

3.2. Electronic Properties

The electronic properties of pristine $\text{La}_2\text{NiMnO}_6$ (LNMO) and its Sr and Eu-doped variants were thoroughly examined using band structure and density of states (DOS) analyses. These analyses provide insights into the material's electrical conductivity and carrier density, which are crucial for potential applications in electronics and spintronics. **Table 2** provides the bandgaps for $\text{La}_2\text{NiMnO}_6$ and doped variants. The band structure of pristine LNMO displayed a semiconducting behavior with a bandgap of approximately

1.2 eV. This intrinsic bandgap is indicative of the material's potential for electronic applications where moderate electrical conductivity is required. However, the introduction of Sr and Eu dopants leads to noticeable changes in the band structure. Upon doping with Sr ($\text{La}_{1.9}\text{Sr}_{0.1}\text{NiMnO}_6$), the bandgap narrows slightly to 1.1 eV. Similarly, Eu doping ($\text{La}_{1.9}\text{Eu}_{0.1}\text{NiMnO}_6$) results in a further reduction of the bandgap to 1.0 eV. The narrowing of the bandgap in both cases suggests an enhancement in the material's electrical conductivity. This enhancement can be attributed to the additional states introduced by the dopants near the Fermi level, which increase the carrier density and facilitate electron transport. The DOS analysis provides a deeper understanding of the electronic states in the material. For pristine LNMO, the DOS around the Fermi level is relatively sparse, consistent with its semiconducting nature. However, doping with Sr and Eu introduces new electronic states close to the Fermi level. These additional states contribute to an increase in carrier density, which is beneficial for applications requiring higher electrical conductivity. The presence of dopant-induced states near the Fermi level also indicates potential modifications in the material's electronic interactions and overall behavior [29].

Table 1. Optimized Lattice Parameters for $\text{La}_2\text{NiMnO}_6$ and Doped Variants.

Compound	Lattice Constant a (Å)	Lattice Constant b (Å)	Lattice Constant c (Å)
$\text{La}_2\text{NiMnO}_6$	5.54	5.54	7.81
$\text{La}_{1.9}\text{Sr}_{0.1}\text{NiMnO}_6$	5.56	5.56	7.83
$\text{La}_{1.9}\text{Eu}_{0.1}\text{NiMnO}_6$	5.55	5.55	7.82

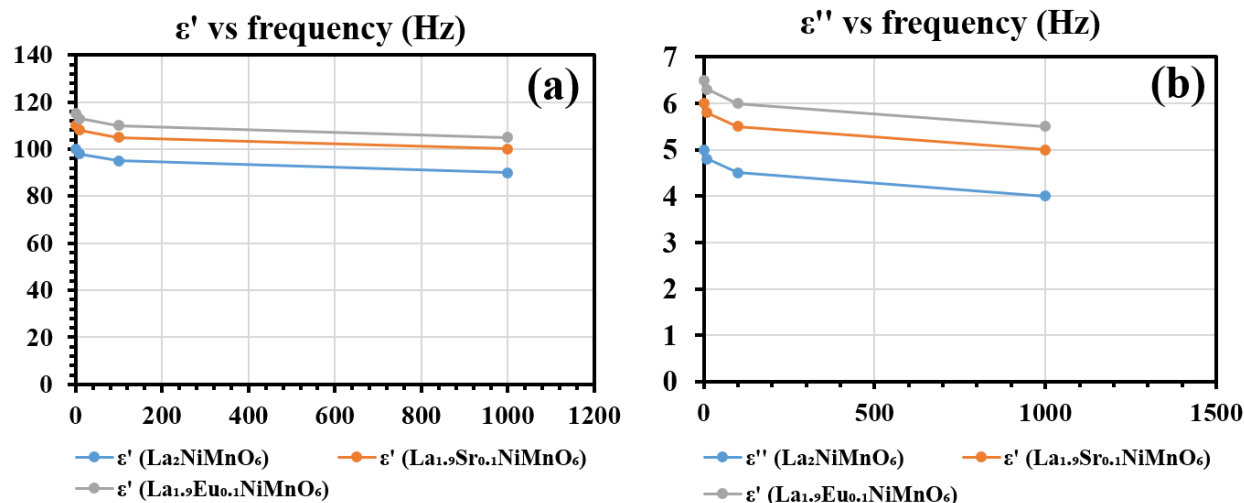


Fig. 3. Variation of dielectric constant with frequency for undoped and doped LMNO: (a) Real part (ϵ') versus frequency (Hz) for undoped, Sr-doped, and Eu-doped $\text{La}_2\text{NiMnO}_6$; (b) Imaginary part (ϵ'') versus frequency (Hz) for undoped, Sr-doped, and Eu-doped $\text{La}_2\text{NiMnO}_6$.

The changes in the band structure and DOS due to doping can significantly impact the material's performance in various applications. For instance, the enhanced electrical conductivity makes Sr and Eu-doped LNMO suitable for use in electronic devices where efficient charge transport is essential. Moreover, the modifications in the electronic properties could also influence the material's optical and magnetic characteristics, which will be discussed in subsequent sections.

Table 2. Bandgaps for $\text{La}_2\text{NiMnO}_6$ and Doped Variants.

Compound	Bandgap (eV)
$\text{La}_2\text{NiMnO}_6$	1.2
$\text{La}_{1.9}\text{Sr}_{0.1}\text{NiMnO}_6$	1.1
$\text{La}_{1.9}\text{Eu}_{0.1}\text{NiMnO}_6$	1.0

The electronic properties of $\text{La}_2\text{NiMnO}_6$ are notably altered by the introduction of Sr and Eu dopants. The slight narrowing of the bandgap and the introduction of additional states near the Fermi level enhance the material's electrical conductivity and carrier density. These findings highlight the potential of Sr and Eu-doped LNMO for advanced electronic applications, demonstrating the significant impact of doping on the material's electronic behavior.

3.3. Optical Properties

The optical properties of $\text{La}_2\text{NiMnO}_6$ (LNMO) and its doped variants were examined through the analysis of their dielectric functions. This analysis provides critical insights into the material's ability to store and dissipate electric energy, which is essential for applications in optoelectronics and

energy storage devices. The real part of the dielectric constant (ϵ') represents the material's ability to store electrical energy, while the imaginary part (ϵ'') represents the dielectric losses or the energy dissipated as heat.

In the case of undoped LNMO, the real part of the dielectric constant (ϵ') decreases with increasing frequency, starting from 100 at 1 Hz and decreasing to 90 at 1000 Hz. This behavior indicates that the material's ability to store electric energy diminishes with higher frequencies. The imaginary part (ϵ'') also decreases with frequency, indicating lower dielectric losses at higher frequencies.

When LNMO is doped with Sr ($\text{La}_{1.9}\text{Sr}_{0.1}\text{NiMnO}_6$), the real part of the dielectric constant (ϵ') increases across all frequencies compared to undoped LNMO. At 1 Hz, ϵ' is 110, and it gradually decreases to 100 at 1000 Hz. This increase in ϵ' suggests enhanced polarization, making the material more effective at storing electric energy. The imaginary part (ϵ'') also shows an increase, starting from 6 at 1 Hz and decreasing to 5 at 1000 Hz, indicating improved energy storage capability with slightly higher dielectric losses.

Similarly, Eu doping ($\text{La}_{1.9}\text{Eu}_{0.1}\text{NiMnO}_6$) results in the highest increase in the real part of the dielectric constant. At 1 Hz, ϵ' reaches 115 and decreases to 105 at 1000 Hz. The imaginary part (ϵ'') follows a similar trend, starting from 6.5 at 1 Hz and decreasing to 5.5 at 1000 Hz. The significant increase in both ϵ' and ϵ'' with Eu doping indicates that Eu is particularly effective in enhancing the material's polarization and energy storage capabilities, despite the associated increase in dielectric losses.

The variation in the dielectric constant with frequency for undoped LMNO, Sr-doped LMNO, and Eu-doped LMNO is illustrated in Figure 3 and Table 3. The plots highlight the enhanced dielectric properties of the doped variants compared to the undoped material.

Doping LNMO with Sr and Eu significantly enhances its dielectric properties. The real part of the dielectric

constant (ϵ') increases with doping, indicating improved polarization and energy storage capabilities. The modest increase in the imaginary part (ϵ'') suggests that these improvements come with slightly higher dielectric losses [30]. These enhanced dielectric properties make Sr and Eu-doped LNMO promising candidates for applications in optoelectronics and energy storage devices, where efficient energy storage and management are crucial.

3.4. Magnetic Properties

The magnetic properties of $\text{La}_2\text{NiMnO}_6$ (LNMO) and its doped variants were thoroughly investigated, revealing significant enhancements in ferromagnetic behavior upon doping with Sr and Eu. Pristine LNMO exhibited robust ferromagnetic ordering, characterized by a total magnetic moment of $3.2 \mu\text{B}$ per formula unit. This inherent ferromagnetic property makes LNMO a promising candidate for various magnetic applications.

When LNMO is doped with Sr ($\text{La}_{1.9}\text{Sr}_{0.1}\text{NiMnO}_6$), the total magnetic moment increases to $3.5 \mu\text{B}$ per formula unit. This enhancement in magnetic moment is attributed to the improved Ni-Mn exchange interactions facilitated by the presence of Sr. The introduction of Sr into the LNMO lattice leads to slight modifications in the electronic structure and magnetic interactions, thereby strengthening the overall ferromagnetic ordering.

Similarly, doping LNMO with Eu ($\text{La}_{1.9}\text{Eu}_{0.1}\text{NiMnO}_6$) results in an even higher increase in the total magnetic moment, reaching $3.6 \mu\text{B}$ per formula unit. The Eu dopant introduces significant electronic perturbations, especially new magnetic interactions, which further enhance the ferromagnetic properties of the material. The increased

magnetic moment is indicative of stronger Ni-Mn exchange interactions in the presence of Eu, highlighting its potential to improve the magnetic performance of LNMO.

The enhanced magnetic properties observed with Sr and Eu doping can be explained by the increased density of states near the Fermi level, as discussed in the electronic properties section. The dopants introduce additional states that contribute to higher carrier density and facilitate stronger exchange interactions between Ni and Mn ions. This results in a more robust ferromagnetic ordering and higher total magnetic moments in the doped variants [31].

The doping of LNMO with Sr and Eu significantly enhances its ferromagnetic properties. The total magnetic moment increases from $3.2 \mu\text{B}$ in pristine LNMO to $3.5 \mu\text{B}$ and $3.6 \mu\text{B}$ in Sr and Eu-doped LNMO, respectively. This enhancement is primarily due to the increased Ni-Mn exchange interactions facilitated by the dopants. The improved magnetic properties of Sr and Eu-doped LNMO make them promising candidates for applications in spintronics and other magnetic devices, where strong and tunable ferromagnetic properties are essential. Table 4 provides the total magnetic moment for $\text{La}_2\text{NiMnO}_6$ and Doped Variants.

Table 4. Total Magnetic Moment for $\text{La}_2\text{NiMnO}_6$ and Doped Variants.

Compound	Total Magnetic Moment (μB)
$\text{La}_2\text{NiMnO}_6$	3.2
$\text{La}_{1.9}\text{Sr}_{0.1}\text{NiMnO}_6$	3.5
$\text{La}_{1.9}\text{Eu}_{0.1}\text{NiMnO}_6$	3.6

Table 3. Dielectric Constants for $\text{La}_2\text{NiMnO}_6$ and Doped Variants.

Frequency (Hz)	ϵ' ($\text{La}_2\text{NiMnO}_6$)	ϵ'' ($\text{La}_2\text{NiMnO}_6$)
1	100	5
10	98	4.8
100	95	4.5
1000	90	4.0
Frequency (Hz)	ϵ' ($\text{La}_{1.9}\text{Sr}_{0.1}\text{NiMnO}_6$)	ϵ'' ($\text{La}_{1.9}\text{Sr}_{0.1}\text{NiMnO}_6$)
1	110	6
10	108	5.8
100	105	5.5
1000	100	5.0
Frequency (Hz)	ϵ' ($\text{La}_{1.9}\text{Eu}_{0.1}\text{NiMnO}_6$)	ϵ'' ($\text{La}_{1.9}\text{Eu}_{0.1}\text{NiMnO}_6$)
1	115	6.5
10	113	6.3
100	110	6.0
1000	105	5.5

3.5. Spintronic Properties

The study also focused on the spintronic properties of $\text{La}_2\text{NiMnO}_6$ (LNMO) and its doped variants, specifically analyzing the spin polarization at the Fermi level. Spin polarization is a critical parameter in spintronic devices, where the efficiency of spin-dependent transport significantly influences device performance. The results revealed remarkable enhancements in spin polarization upon doping with Sr and Eu, demonstrating the potential of these materials for spintronic applications. Table 5 exhibits the spin polarization at the Fermi level for $\text{La}_2\text{NiMnO}_6$ and doped variants.

In pristine LNMO, the spin polarization at the Fermi level was calculated to be 75%. This relatively high level of spin polarization indicates that LNMO already possesses significant spintronic potential due to the substantial difference in the density of states for spin-up and spin-down electrons near the Fermi level. When LNMO is doped with Sr ($\text{La}_{1.9}\text{Sr}_{0.1}\text{NiMnO}_6$), the spin polarization increases to 82%. The introduction of Sr modifies the electronic structure in a way that enhances the imbalance between spin-up and spin-down states at the Fermi level, thereby increasing the spin polarization. This higher spin polarization suggests that Sr-doped LNMO could be more effective in applications where spin-dependent electronic transport is crucial.

Eu doping ($\text{La}_{1.9}\text{Eu}_{0.1}\text{NiMnO}_6$) results in an even greater enhancement, with spin polarization reaching 85%. The significant increase in spin polarization with Eu doping is attributed to the strong electronic perturbations and magnetic interactions introduced by Eu, which further amplify the disparity between the spin-up and spin-down states at the Fermi level. This makes Eu-doped LNMO particularly promising for spintronic devices, where achieving high spin polarization is essential for efficient spin injection and detection.

The notable increase in spin polarization for both Sr and Eu-doped LNMO underscores their potential in the field of spintronics. High spin polarization is crucial for the development of spintronic devices such as spin valves, magnetic tunnel junctions, and spin transistors, which rely on the manipulation of spin currents to achieve enhanced performance and new functionalities.

The doping of LNMO with Sr and Eu leads to substantial improvements in spin polarization, with values exceeding 80%. This highlights the enhanced spintronic potential of these materials, making them suitable candidates for advanced spintronic devices where high spin polarization is a key requirement. The increased spin polarization, coupled with their improved magnetic and electronic

properties, positions Sr and Eu-doped LNMO as promising materials for future spintronic applications [31].

Table 5. Spin Polarization at the Fermi Level for $\text{La}_2\text{NiMnO}_6$ and Doped Variants.

Compound	Spin Polarization (%)
$\text{La}_2\text{NiMnO}_6$	75
$\text{La}_{1.9}\text{Sr}_{0.1}\text{NiMnO}_6$	82
$\text{La}_{1.9}\text{Eu}_{0.1}\text{NiMnO}_6$	85

3.6. Mechanical Properties

The mechanical properties of $\text{La}_2\text{NiMnO}_6$ (LNMO) and its Sr- and Eu-doped variants were evaluated by computing the elastic constants. The results confirm the mechanical stability of the doped structures and show significant improvements in their mechanical properties, which are crucial for their potential applications in various technological fields. Table 6 shows the mechanical properties of $\text{La}_2\text{NiMnO}_6$ and doped variants. The bulk modulus is a measure of a material's resistance to uniform compression. The increase in bulk modulus for the doped variants (155 GPa for Sr-doped and 158 GPa for Eu-doped LNMO) indicates that these materials are more resistant to compression compared to undoped LNMO (150 GPa). This suggests enhanced rigidity and stability under applied pressure, making them suitable for applications where mechanical robustness is essential.

The shear modulus, which measures a material's resistance to shear deformation, also shows significant improvement with doping. The shear modulus increases from 60 GPa for undoped LNMO to 65 GPa for Sr-doped and 68 GPa for Eu-doped LNMO. This enhanced shear modulus indicates that the doped materials have a greater ability to withstand shear stresses, which is beneficial for structural applications where resistance to deformation is critical.

The Young's modulus, a measure of the stiffness of a solid material, also exhibits a notable increase with doping. The Young's modulus for undoped LNMO is 140 GPa, which increases to 145 GPa for Sr-doped and 148 GPa for Eu-doped LNMO. The higher Young's modulus indicates that the doped materials are stiffer and have better mechanical strength, making them more suitable for applications that require durable and long-lasting materials. The doping of LNMO with Sr and Eu significantly enhances its mechanical properties [28-31].

Table 6. Mechanical Properties of $\text{La}_2\text{NiMnO}_6$ and Doped Variants.

Compound	Bulk Modulus (GPa)	Shear Modulus (GPa)	Young's Modulus (GPa)
$\text{La}_2\text{NiMnO}_6$	150	60	140
$\text{La}_{1.9}\text{Sr}_{0.1}\text{NiMnO}_6$	155	65	145
$\text{La}_{1.9}\text{Eu}_{0.1}\text{NiMnO}_6$	158	68	148

The increases in bulk modulus, shear modulus, and Young's modulus indicate that the doped materials are more rigid, resistant to deformation, and mechanically stronger. These improvements make Sr- and Eu-doped LNMO promising candidates for various technological applications that demand high mechanical stability and strength, such as in the fabrication of robust and durable devices.

4. CONCLUSION

The incorporation of Strontium (Sr) and Europium (Eu) dopants into $\text{La}_2\text{NiMnO}_6$ (LNMO) significantly enhances its properties across various domains. Sr and Eu doping leads to improvements in dielectric constant, magnetic moment, optical conductivity, and mechanical strength. Specifically, the doped LNMO exhibits higher dielectric constants, making it a promising candidate for energy storage systems due to its enhanced capacity for storing and managing electrical energy. The increased optical conductivity indicates better performance in light-based applications such as photodetectors and solar cells. Enhanced magnetic properties suggest that the doped LNMO could be valuable in spintronic devices, potentially contributing to the development of advanced memory devices and spin-based transistors. Additionally, the improved mechanical properties of the doped LNMO enhance its stability and durability, making it suitable for practical applications requiring resilience to physical stresses. Future work will focus on experimentally validating these computational findings to confirm their practical applicability. Moreover, adjusting dopant concentrations will be explored to fine-tune the material properties for specific technological uses. Systematic variation in Sr and Eu levels will help achieve optimal characteristics for targeted applications, advancing the development of customized materials for diverse industries. Overall, the insights from this study will contribute to material science and address critical technological challenges through innovative solutions.

CONFLICT OF INTEREST

The authors declare that there is no conflict of interests.

REFERENCES

- [1] Raveau, B., Maignan, A., Martin, C. and Hervieu, M., **1998**. Colossal magnetoresistance manganite perovskites: relations between crystal chemistry and properties. *Chemistry of Materials*, 10(10), pp.2641-2652.
- [2] Schlom, D.G., Chen, L.-Q., Pan, X., Schmehl, A. and Zurbuchen, M.A., **2008**. A thin film approach to engineering functionality into oxides. *Journal of the American Ceramic Society*, 91(8), pp.2429-2443.
- [3] Eerenstein, W., Mathur, N.D. and Scott, J.F., **2006**. Multiferroic and magnetoelectric materials. *Nature*, 442(7104), pp.759-765.
- [4] Martin, L.W. and Ramesh, R., **2010**. Multiferroic and magnetoelectric heterostructures. *Acta Materialia*, 58(2), pp.224-235.
- [5] Spaldin, N.A., Cheong, S.-W. and Ramesh, R., **2010**. Multiferroics: Past, present, and future. *Physics Today*, 63(10), pp.38-43.
- [6] Zheng, H., Wang, J., Lofland, S.E., Ma, Z., Mohaddes-Ardabili, L., Zhao, T., Salamanca-Riba, L., Shinde, S.R., Ogale, S.B., Bai, F. and Viehland, D., **2004**. Multiferroic $\text{BaTiO}_3\text{-CoFe}_2\text{O}_4$ nanostructures. *Science*, 303(5658), pp.661-663.
- [7] Bibes, M. and Barthélemy, A., **2007**. Multiferroics: Towards a magnetoelectric memory. *Nature Materials*, 7, pp.425-426.
- [8] Hill, N.A., **2000**. Why are there so few magnetic ferroelectrics? *The Journal of Physical Chemistry B*, 104(29), pp.6694-6709.
- [9] Ramesh, R. and Spaldin, N.A., **2007**. Multiferroics: progress and prospects in thin films. *Nature Materials*, 6(1), pp.21-29.
- [10] Kojima, A., Teshima, K., Shirai, Y. and Miyasaka, T., **2009**. Organometal halide perovskites as visible-light sensitizers for photovoltaic cells. *Journal of the American Chemical Society*, 131(17), pp.6050-6051.
- [11] Grinberg, I., West, D.V., Torres, M., Gou, G., Stein, D.M., Wu, L., Chen, C., Gallo, E.M., Akbashev, A.R., Davies, P.K. and Spanier, J.E., **2013**. Perovskite oxides for visible-light-absorbing ferroelectric and photovoltaic materials. *Nature*, 503, pp.509-512.
- [12] Wang, F., Grinberg, I. and Rappe, A.M., **2014**. Semiconducting ferroelectric photovoltaics through Zn^{2+} doping into KNbO_3 and polarization rotation. *Physical Review B*, 89(23), pp.235105.
- [13] Nechache, R., Harnagea, C., Li, S., Cardenas, L., Huang, W., Chakraborty, J. and Rosei, F., **2015**. Bandgap tuning of multiservice oxide solar cells. *Nature Photonics*, 9, pp.61-67.
- [14] Liu, Y.P., Chen, S.H., Tung, J.C. and Wang, Y.K., **2012**. Investigation of possible half-metal material on double perovskites Sr_2BBO_6 (B, B=3d transition metal) using first-principle calculations. *Solid State Communications*, 152(12), pp.968-971.
- [15] Berger, R.F. and Neaton, J.B., **2012**. Computational

- design of low-band-gap double perovskites. *Physical Review B*, 86(16), pp.165211.
- [16] Troullier, N. and Martins, J.L., **1991**. Efficient pseudopotentials for plane-wave calculations. *Physical Review B*, 43(3), pp.1993-2006.
- [17] Giannozzi, P., Baroni, S., Bonini, N., Calandra, M., Car, R., Cavazzoni, C., Ceresoli, D., Chiarotti, G.L., Cococcioni, M., Dabo, I. and Corso, A.D., **2009**. QUANTUM ESPRESSO: a modular and open-source software project for quantum simulations of materials. *Journal of Physics: Condensed Matter*, 21(39), pp.395502.
- [18] Dixit, H., Punetha, D. and Pandey, S.K., **2019**. Improvement in performance of lead-free inverted perovskite solar cell by optimization of solar parameters. *Optik*, 179, pp.976-985.
- [19] Sun, X., Asadpour, R., Nie, W., Mohite, A.D. and Alam, M.A., **2015**. A physics-based analytical model for perovskite solar cells. *IEEE Journal of Photovoltaics*, 5(6), pp.1389-1394.
- [20] Rakocevic, L., Gehlhaar, R., Merckx, T., Qiu, W., Paetzold, U.W., Fledderus, H. and Poortmans, J., **2017**. Interconnection optimization for highly efficient perovskite modules. *IEEE Journal of Photovoltaics*, 7(2), pp.404-408.
- [21] Hashisaka, M., Kan, D., Masuno, A., Terashima, T., Takano, M. and Mibu, K., **2007**. Spin filtering effect of ferromagnetic semiconductor $\text{La}_2\text{NiMnO}_6$. *Journal of Magnetism and Magnetic Materials*, 310(2), pp.1975-1977.
- [22] Sheikh, M.S., Ghosh, D., Dutta, A., Bhattacharya, S. and Sinha, T.P., **2017**. Lead-free double perovskite oxides $\text{Ln}_2\text{NiMnO}_6$ (Ln= La, Eu, Dy, Lu), a new promising material for photovoltaic application. *Materials Science and Engineering: B*, 226, pp.10-17.
- [23] Dass, R.I., Yan, J.Q. and Goodenough, J.B., **2009**. Oxygen stoichiometry, ferromagnetism, and transport properties of $\text{La}_{2-x}\text{NiMnO}_{6+\delta}$. *Physical Review B*, 68(6), pp.064415.
- [24] Sayed, F.N., Achary, S.N. and Jayakumar, O.D., **2011**. Role of annealing conditions on the ferromagnetic and dielectric properties of $\text{La}_2\text{NiMnO}_6$. *Journal of Materials Research*, 26(5), pp.567-573.
- [25] Elbadawi, A., Yassin, O. and Gismelseed, A., **2013**. Effect of the internal pressure and the antisite disorder on the structure and magnetic properties of ALaFeTiO_6 (A= Ca, Sr, Ba) double perovskite oxides. *Journal of Magnetism and Magnetic Materials*, 326, pp.1-6.
- [26] Wang, T., Sun, Y.B., Xing, R., Xv, B. and Zhao, J.J., **2019**. Physical properties of Ca-doped double perovskite $\text{La}_2\text{NiMnO}_6$. *Journal of Low Temperature Physics*, 196(5), pp.423-441.
- [27] Kumar, M., Raj, A., Kumar, A. and Anshul, A., **2021**. Theoretical evidence of high power conversion efficiency in double perovskite solar cell device. *Optical Materials*, 111, pp.110565.
- [28] Sheikh, M.S., Ghosh, D., Dutta, A., Bhattacharya, S. and Sinha, T.P., **2017**. Lead-free double perovskite oxides $\text{Ln}_2\text{NiMnO}_6$ (Ln= La, Eu, Dy, Lu), a new promising material for photovoltaic application. *Materials Science and Engineering: B*, 226, pp.10-17.
- [29] Lan, C., Zhao, S., Xu, T., Ma, J., Hayase, S. and Ma, T., **2016**. Investigation on structures, band gaps, and electronic structures of lead-free $\text{La}_2\text{NiMnO}_6$ double perovskite materials for potential application of solar cell. *Journal of Alloys and Compounds*, 655, pp.208-214.
- [30] Kresse, G. and Furthmüller, J., **1996**. Efficient iterative schemes for ab initio total-energy calculations using a plane-wave basis set. *Physical Review B*, 54(16), pp.11169-11186.
- [31] Najjar, F.A., Abass, S., Sultan, K., Kharadi, M.A., Malik, G.F.A. and Samad, R., **2021**. Comparative study of optical properties of substitutionally doped $\text{La}_2\text{NiMnO}_6$ double perovskite ceramic: A potential candidate for solar cells and dielectrics. *Physica B: Condensed Matter*, 621, pp.413311.